Palaeontologia Electronica
http://palaeo-electronica.org

Multi-view stereo three-dimensional reconstruction of lower molars of Recent and Pleistocene rhinoceroses for mesowear analysis

Elina Hernesniemi, Kasimir Blomstedt, and Mikael Fortelius

ABSTRACT

In this work we tested how well a method, where 3D reconstructions are produced from photographs, is suited for palaeontological investigations. This method is attractive since photographing specimens is faster than scanning them with a needle or a laser scanner, which means that for example museum visits can be better utilised. Also, a digital camera is far less expensive and more mobile than dedicated 3D scanners. The palaeodiet reconstruction of North-Western European Pleistocene rhinoceroses was used as a test case. For this purpose we developed a method for the analysis of lower molars of rhinoceroses, to which classical mesowear analysis cannot be applied. This method is based on examining the facets of the buccal enamel band. We considered two variations of the method. In the first variant we digitally measured the angle between the surface of the enamel edge and the buccal side surface of the teeth and used it to score the wear patterns. The second variant was based on a visual scoring. Our experience suggests that the 3D models based on digital photographs provide sufficient accuracy for the models to be suitable for palaeontological investigations. The results suggest that the dietary regime of *Stephanorhinus hundsheimensis* and *Stephanorhinus kirchbergensis* fall within the browsing realm. The diet of *Stephanorhinus hemitoechus* was more abrasive, but not as abrasive as that of the Recent mixed feeder *Rhinoceros unicornis*. The dietary regime of *Coelodonta antiquitatis* falls between the dietary regimes of the Recent extreme grazer *Ceratotherium simum* and mixed feeder *Rhinoceros unicornis*.

Elina Hernesniemi. Department of Geosciences and Geography, University of Helsinki, PO Box 64, FIN-00014 University of Helsinki, Finland. elina.hernesniemi@helsinki.fi
Kasimir Blomstedt. Department of Cell Biology and Anatomy, Laboratory of Biophysics, University of Turku, FIN-20520 Turku, Finland. kasimir.blomstedt@utu.fi
Mikael Fortelius. Department of Geosciences and Geography; Institute of Biotechnology, University of Helsinki, PO Box 64, FIN-00014 University of Helsinki, Finland. mikael.fortelius@helsinki.fi

Key Words: 3D; mesowear; molar teeth, lower; rhinoceros; Pleistocene

PE Article Number: 14.2.2T

Submission: 6 July 2010. Acceptance: 18 March 2011

Hernesniemi, Elina, Blomstedt, Kasimir, and Fortelius, Mikael. 2011. Multi-view stereo 3D reconstruction of lower molars of Recent and Pleistocene rhinoceroses for mesowear analysis. *Palaeontologia Electronica* Vol. 14, Issue 2; 2T:15p; palaeo-electronica.org/2011_2/246/index.html

INTRODUCTION

In the present-day study of palaeontology, new technology, such as 3D modelling, is increasingly utilized. Powerful computers and digital 3D models of fossils enable many new research projects. However, 3D scanners tend to be rather expensive and may not be accessible to all researchers. Also, unless the 3D scanner is very portable, it may be difficult to use one in field conditions or during museum visits.

The purpose of this work is to test how well a method, in which 3D models are produced from ordinary digital photographs, works for palaeontological studies. The great advantage of this kind of method is that all that is needed for generating 3D models is an ordinary digital camera and a computer for post-processing. Hence, the method can be used whenever it is possible to take photographs, because no special 3D scanners are needed.

In this work we studied the dietary regimes of Pleistocene rhinoceros species as a test case. We analysed dental fossils of four Pleistocene rhinoceros species from North-Western Europe, *Stephanorhinus kirchbergensis* (Jäger, 1839), *S. hemitoechus* (Falconer, 1868), *S. hundsheimensis* (Toula, 1902), and *Coelodonta antiquitatis* (Blumenbach, 1799). In the last couple of years these species have been the subject of a vivid discussion (among others Lacombat 2006a, 2006b, 2007; Billia 2007, 2008a, 2008b; Koenigswald et al. 2007; Kahlke and Lacombat 2008; Tong and Wu 2010; Kahlke and Kaiser 2010). Our intention was to find out whether wear patterns of lower molars of rhinoceroses could be used for mesowear analysis. We compared the reconstructed palaeodiets of the Pleistocene species to the dietary regimes of the five Recent species, *Diceros bicornis* (Linnaeus, 1758), *Ceratotherium simum* (Burchell, 1817), *Rhinoceros unicornis* (Linnaeus, 1758), *R. sondaicus* (Desmarest, 1822) and *Dicerorhinus sumatrensis* (Fischer, 1814).

Mesowear analysis is a method, which can be used to reconstruct the diets of ungulate species (Fortelius and Solounias 2000). The method is based on facet development on the occlusal surfaces of upper cheek teeth. Mesowear is recorded by examining the shape of adequately worn cusp apices macroscopically to estimate the relative amount of abrasive (food on tooth) and attritive (tooth on tooth) wear. Leaf browsing tends to result in an attritive wear pattern, where the cusp apices are sharp, whereas more abrasive grazing tends to result in blunt cusp apices.

Originally Fortelius and Solounias (2000) employed only second upper molars for mesowear analysis, but later the method was also extended to the analysis of other upper cheek teeth of ruminants, horses and rhinoceroses, as well as to the analysis of the lower cheek teeth of horses and ruminants (see Franz-Odentaal and Kaiser 2003; Kaiser and Fortelius 2003; Kaiser and Solounias 2003; Kaiser and Rössner 2007; Kahlke and Kaiser 2010). However, the classical mesowear analysis does not lend itself to the study of lower cheek teeth of rhinoceros species. Restricting analyses only to the upper teeth of rhinoceroses limits the use of the method, as the fossil assemblages contain both upper and lower teeth.

In this study we analysed the upper molars (M2 and M1) of rhinoceros species using the classical mesowear analysis. For lower molars (m2 and m1) we used two different methods, and both are based on analysing the wear patterns, that is, the facet development of the buccal enamel band. Facets develop during occlusion strokes when lower teeth are in contact with upper teeth, i.e., in attrition (see for example Butler 1972; Fortelius 1985; Fortelius and Solounias 2000). Abrasion does not lead to facet development. As a result, the profile of buccal enamel edges of the lower molars of separate species tend to be rather different, as can be seen in Figure 1. In the first method, we digitally measured the angle between the buccal side surface and the surface of the enamel edge from the 3D reconstructions. In the second method, on the other hand, we visually categorized the teeth into two groups; those with facets and those without facets.

The dietary regimes of the Pleistocene rhinoceros species have raised questions for a long time. Especially the diet of the species *Stephanorhinus hemitoechus* has been a controversial issue. Earlier *S. hemitoechus* has been seen as a grass consuming steppe rhino (see for example Zeuner 1934; Loose 1975), whereas in later studies a grazing diet has been considered as highly improbable (Fortelius 1982; Fortelius et al. 1993). Since all the *Stephanorhinus* Kretzoi, 1942 species studied here seem to occasionally have occupied the same areas (for example, fossils of all the three species have been found at Mosbach, see Fortelius et al. 1993), the possible differences in their dietary regimes are very interesting. The woolly rhino, *Coelodonta antiquitatis,* has for a long time been considered a cold adapted grazing animal, whose winter diet might have been different from its summer diet (Loose 1975).

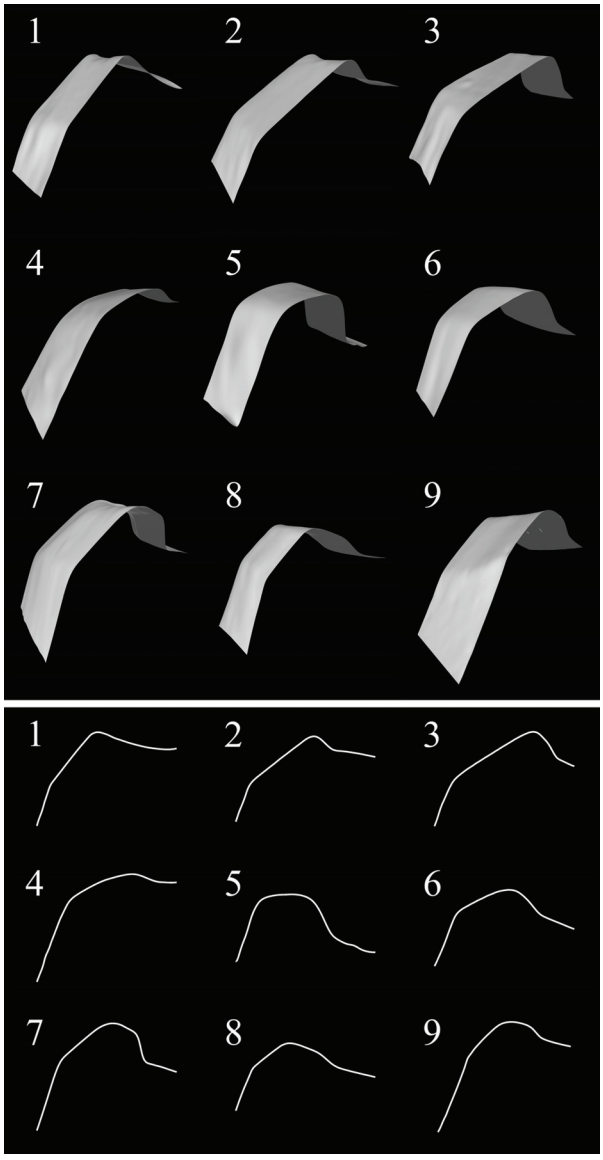

FIGURE 1. (Upper part) Surface profiles of buccal lower teeth enamel edges from the hypoconid tip regions of m2s. (Lower part) The on-edge curves corresponding to the surface profiles. 1. *S. kirchbergensis* BMNH-19841; 2. *S. hundsheimensis* BMNH-M.19428; 3. *S. hemitoechus* BMNH-M.36620; 4. *C. antiquitatis* BMNH-M.89; 5. *C. simum* BMNH-1967.8.31.2; 6. *R. unicornis* BMNH-72.739; 7. *R. sondaicus* NHMD-CN28; 8. *D. sumatrensis* BMNH-1921.2.8.2; 9. *D. bicornis* FMNH-945/1960.

Institutional abbreviations

BMNH British Museum of Natural History, London
FMNH Finnish Museum of Natural History, Helsinki
NHMD Zoological Museum, Natural History Museum of Denmark, University of Copenhagen, Copenhagen
RMCA Royal Museum for Central Africa, Tervuren
UUZM Uppsala University, the Museum of Evolution, Uppsala

MATERIAL

The dental material of four Pleistocene rhinoceros species, *Stephanorhinus kirchbergensis*, *S. hemitoechus*, *S. hundsheimensis*, and *Coelodonta antiquitatis,* were studied and compared to the dental material of the five Recent rhinoceros species, *Diceros bicornis*, *Ceratotherium simum*, *Dicerorhinus sumatrensis*, *Rhinoceros sondaicus*, and *R. unicornis*. All the studied dental fossils come from the fossil localities of Britain and are housed in BMNH. The early middle and middle Pleistocene species *S. hundsheimensis* from the British Isles has traditionally been assigned to *S. etruscus* (Falconer, 1868). The morphological differences between *S. hundsheimensis* and *S. etruscus* are rather small, and their separation based only on isolated teeth or dentitions, which are used in this study, is difficult or even impossible (see Fortelius et al. 1993; Lacombat 2006a, 2006b). However, here we follow Fortelius et al. (1993) who suggested that all the European "etruscoid" rhinoceroses from the early middle Pleistocene can be referred to *S. hundsheimensis* (see also Mazza 1988 for description of *S. etruscus*).

The Recent rhinoceros specimens studied are housed in BMNH, FMNH, NHMD, RMCA, and UUZM. Only specimens belonging to wild-shot animals were used in this study. The Recent *Ceratotherium* (Gray, 1868) was treated as one species, instead of dividing it to *C. simum* and *C. cottoni* as suggested by Groves et al. (2010). Both the second and the first upper and lower molars were used in this study. Unworn teeth as well as teeth in very early or in very late wear stage were excluded. All the adequately worn upper and lower molars (M2, M1, m2, and m1) from each individual were used in all analyses except for the angle measurement analysis, in which only one lower molar of each individual animal was included. From each species upper and lower molars of ten or more individuals were studied, except for *D. sumatrensis*, from which lower molars were studied only from seven individuals. The dental material used in this study is shown in Appendix.

METHODS

Polysiloxane putty (Lab-Putty, Coltène/Whaledent AG, Altstätten, Switzerland) was used to make partial moulds of the lower molars (m2 and m1) after which synthetic dental stone (Fujirock by GC Europe n.v., Leuwen, Belgium) was used to make replicas. Statistical calculations were carried out using the statistics package JMP 8.0.2 (SAS Insti-

tute, Inc., Cary, North Carolina, USA), except for the bar graphs and hierarchical clustering, which were produced in MATLAB (Version 6.5.0. 180913a Release 13, The MathWorks, Inc.). Euclidean distance and complete linkage were used in the hierarchical clustering.

Mesowear Analysis of Upper Molars

The original mesowear method, in which cusp apices were visually scored as sharp, rounded, or blunt, and the valleys as high or low (Fortelius and Solounias 2000), was applied for the first and second upper molars. Only sharper apices were scored. The index of hypsodonty (Janis 1988) was excluded from this study. A hierarchical cluster analysis of the mesowear data of the upper molars was performed. In this analysis, following Fortelius and Solounias (2000, figure 2b), we used the relative sharpness, the relative bluntness, and the relative height of the molar cusps as variables.

Wear Pattern Analyses of Lower Molars

For the analysis of the lower molars, we constructed digital 3D models of those parts of the molars that are relevant in the methods used. We used two different methods for the analysis of the lower molars. In the first method the angle between the buccal side surface and the enamel edge was measured, whereas the second method was based on a visual inspection of the buccal side enamel edge, used to determine the presence of facets.

Obtaining 3D representations. To be able to analyse the specimens off-line or by computer, we had to obtain digital 3D representations of the teeth. The 3D representations were mostly determined from casts, but teeth from Recent species as well as fossilized teeth were also used as starting points.

The technique we used for obtaining the 3D models is based on an idea where multiple ordinary (2D) photographs showing the target object from different directions are computationally combined to yield a 3D representation of that object. This so-called multi-view stereo (MVS) technique is much faster and more convenient to apply in a field setting than, say, the use of, for example, a needle scanner or a laser scanner. It, however, provides a somewhat lower resolution for the representation. Hence, in order to get some idea of the actual resolution, we have compared the representations obtained by MVS to the representations obtained by a needle scanner and a laser scanner.

For the 3D reconstruction computations we used the combination of two computer programs, Bundler (version 0.3) (Snavely et al. 2006; http://phototour.cs.washington.edu/bundler/) and PMVS (Patch-based Multi-View Stereo Software, version 1) (Furukawa and Ponce 2007; http://grail.cs.washington.edu/software/pmvs/pmvs-1/index.html). The former program was used to estimate the camera parameters (focal length, relative location of camera to specimen, and in what direction the camera was pointed), and the latter program was used to obtain the 3D reconstruction.

Typically some 40 photographs were taken of the same specimen in order to obtain an adequate 3D model. While experimenting with the process, it became clear that the Bundler-PMVS combination requires that care has to be taken both in photographing the specimen as well as in appropriate pre-processing of the images. Indeed, for the programs to be able to find the needed common features more or less uniquely from the different photographs, it was necessary to ensure that the interesting parts of each photograph were in focus and well lit. This mandated that external lighting had to be used together with a long focal length setting on the camera, and furthermore, that the most out-of-focus parts of the photographs were masked. In addition, masking was also used to single-out the interesting parts of each photograph, that is, the parts showing those features of each tooth we were interested in. This was done, because experience showed that for the programs not to hang when processing high-resolution images, the total number of pixels in each image had to be limited. Finally, for the algorithms used by the programs to work, it was also necessary to ensure that there were sufficiently many common details or features that span a number of the photographs. That is, when going from one image to the next (in order), there has to be a sufficient number of common features in each image pair.

The photographs were taken with two different cameras, a Nikon D70 with an AF Micro-Nikkor 60 mm lens and with a Nikon Coolpix 4500. The specimens were placed on a table and secured in place by plasticine. They were illuminated by a pair of 150W construction-site lanterns, which were kept in fixed positions with respect to the table and to the specimen between the photographs. The lights were fixed in place, because as the 3D reconstruction is based on finding common features across a stack of images, it is necessary to ensure that the apparent surface texture, including highlights and shadows, is stationary across all of the photographs. This issue becomes apparent when trying to use the procedure to obtain 3D models from

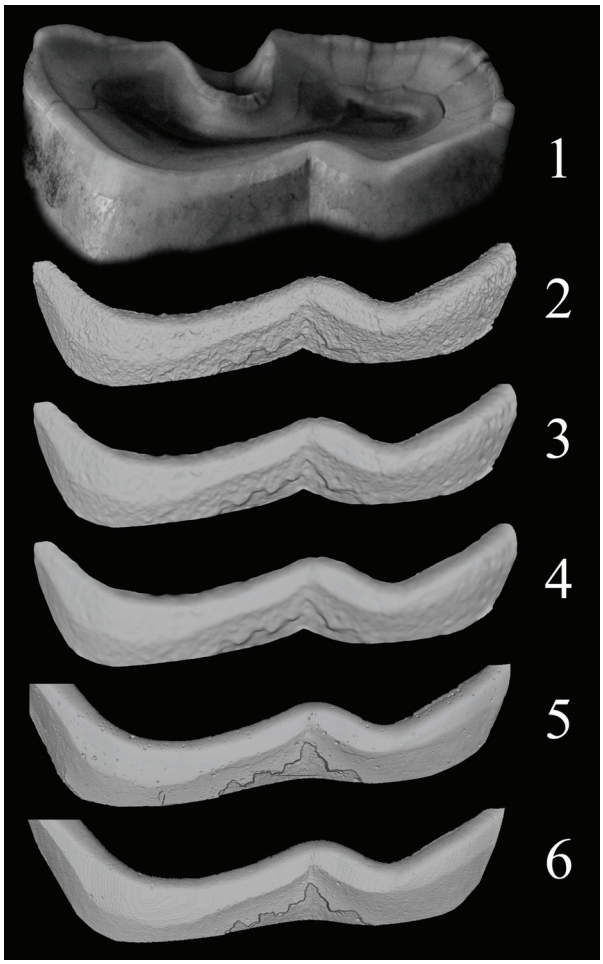

FIGURE 2. Comparison of the models corresponding to the buccal side enamel edge of *D. bicornis* FMNH-945/1960. 1. photograph of the upper part of m2d; 2. photograph-based 3D model before smoothing; 3. photograph-based 3D model after 3 steps of smoothing; 4. photograph-based 3D model after 7 steps of smoothing and after vertex removal; 5. 3D model from laser scanner (30 µm nominal resolution); 6. 3D model from needle scanner (50 µm nominal resolution).

photographs of actual teeth, which typically are quite shiny. The specular reflection implied by the shine means that a part of the surface texture consists of the mirror-image of the environment, especially of the light source(s). This mirror-image by its very nature "wanders" around when the point of view is changed. As a consequence, and since all highlights resemble each other and represent (over)prominent features in the photographs, highlights tend to throw off the 3D reconstruction procedure. To overcome these difficulties, a diffuser (a sheet of baking paper) was introduced between the lights and the specimen when photographing actual teeth.

Once a stack of photographs of a specimen had been obtained, these images were fed to the Bundler program, which returns the camera parameters associated with each image. It also *undistorts* (tries to undo geometrical distortions originating in the camera optics) each image. The masking of the images to only retain in-focus regions of interest was done to the undistorted images, and a set of masks corresponding to each image was thus generated. This masking was done by hand. The undistorted images, their masks, and the associated camera parameters were then passed on to the PMVS program, which used them to build the 3D model. The output from the PMVS program is a set of patches in three-dimensional space. To get more flexibility in the choice of tools used to further process the models, we used the conversion programs "patch2pset.exe" and "PoissonRecon.32.exe", provided with the PMVS software distribution, to convert the patch-based model into a point cloud representation -based mesh. The point cloud essentially contains the three-dimensional coordinates of a huge number of points that PMVS has determined define (lie on) the surface of the specimen.

The 3D point cloud representation of the specimen was then further processed by the Meshlab software (Meshlab v1.2.1.1, Visual Computing Lab–ISTI–CNR [http://meshlab.sourceforge.net/]). First of all, those parts of the representation, which did not represent regions of interest, including the artificial features introduced by PoissonRecon.32.exe when creating the mesh, were cut away from the 3D model. Because the 3D model produced by the PMVS program tends to be rather noisy (see Figure 2), the model was then smoothed by applying the Laplacian smooth –algorithm of Meshlab with parameter 10 seven times in a row to the model. We note that careful smoothing of a noisy model does not really alter the available true information, but rather changes the shape of the erroneous deviations into a visually more pleasing form. Once the model was smoothed, its vertex (point) count was reduced by removing those vertices that lie so close together as to almost providing no additional detail. The procedure was performed with the Merge close vertices – algorithm of Meshlab, with parameter 10. The vertex reduction makes the model more usable in other programs (it leads to a smaller memory usage and decreased processing times). The progress of the smoothing procedure and the subsequent vertex removal is represented in Figure 2, which depicts the result

after 0, 3, and 7 smoothing steps, and after the vertex removal, respectively.

For comparison the results obtained by a needle scanner (Roland Picza PIX-4 3D, 50 µm nominal resolution) and a laser scanner (Nextec Hawk 3D laser scanner, 30 µm nominal resolution) of the same specimen, as well as a photograph taken from roughly the same direction as the models are rendered, are also presented in Figure 2. From the figure it is clear that the results of the needle scanner and the laser scanner provide somewhat more detail than the photograph-based reconstruction. However, more important for our present purpose is the fact that this comparison shows that the detail present in the MVS reconstruction, including the smoothing and vertex removal procedures, faithfully represents the specimen. The reconstruction can therefore, within the accuracy provided by it, be used to reliably analyse the specimen.

Analysing the angles. We measured the angle between the buccal side enamel edge and the buccal surface of molars. In browsers, where the enamel edge tends to develop a facet, this angle is larger than in grazers, where no facets develop. We investigated the lower molars m1 and m2, and measured the angle at two locations, in the vicinity of the hypoconid and protoconid tip regions. That is, approximately at the common edge of the facets one and two, and the facets six and seven (facet numbering according to Butler 1952), respectively. This choice of measurement location was dictated by practical reasons, since it made it relatively easy to measure the angles in a consistent manner for different molars.

The measurements were done on the reconstructed 3D models. For this purpose we used the VRMesh software (VRMesh v.4.1.2 Studio, Copyright 2003-2008, Virtual Grid Company). In order to measure the angle, we first chose a suitable section of the region around the hypoconid or protoconid tip. We then selected two closely spaced points on the boundary edge of the facet or on the enamel edge, depending on whether the molar had a facet or not. The line passing through these two points (indicating the direction of the edge) was then interpreted as the normal of a plane, which bisects the model and lies (roughly) perpendicular to the edge (see Figure 3.1). Next we delete those parts of the model that lay on one side of this plane, thus revealing the surface profile around the edge, as is shown in Figure 3.2. The model was then rotated so that the aforementioned normal coincided with the direction of viewing in VRMesh (see Figure 3.3-4). This rotation produced an effective 2D representation of the surface profile and especially of the angle between the buccal side enamel edge and the buccal surface. Finally, we used the tools provided in VRMesh to measure the angle (alpha) from this 2D representation (see Figure 3.4).

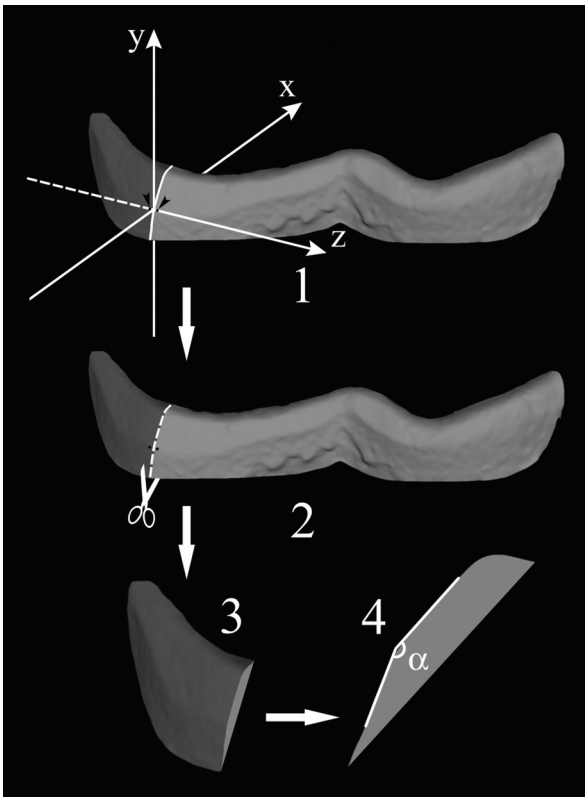

FIGURE 3. Measuring the angle between the buccal side surface and the buccal side enamel edge (FMNH-945/1960, *D. bicornis*). 1. line representing the direction of the enamel edge (normal of bisecting plane); 2. half the model, after bisection; 3. the remaining model is zoomed and rotated so that the normal coincides with the viewing direction; 4. measurement of the angle alpha.

Visual analysis. We also analysed the lower molars visually. In this analysis the molars were divided into groups based on the number of buccal side enamel edges with facets. The presence of facets was determined by visual inspection. We used two kinds of groupings or variations of this method.

In the first variation we determined the presence of the four enamel edge facets, one, two, six, and seven separately, and computed the total number of facets present. This variation thus yields a number between 0 and 4, with 0 indicating that no facets are present, and 4 indicating that facets are

FIGURE 4. Visual inspection of facets. 1. all facets present, number of facets is 4 (BMNH-M.19429, *S. hundsheimensis*); 2. facet 7 absent, number of facets is 3 (BMNH-M.1948, *S. hundsheimensis*); 3. no facets present, number of facets 0 (BMNH-25.5.23.1, *C. simum*).

present everywhere on the enamel edge (see Figure 4).

In the second, simpler, variation we classified the lower molars into two groups, those with at least one buccal facet, and those with no buccal facets. Thus a molar was classified as facetted if any of the facets one, two, six, seven, or any combination thereof was present, otherwise it was classified as not facetted.

RESULTS

In Figure 5 we display the data obtained from the classical mesowear analysis of the upper molars. The result of the hierarchical cluster analysis is shown in Figure 6. We observe that the cusps of the Recent extreme grazer *Ceratotherium simum* are low and almost exclusively blunt. In the fossil species *Coelodonta antiquitatis* the cusps are also mainly low and mostly blunt and rounded, but other kinds of cusps are also present in small numbers. In the Recent graze-dominated mixed feeder *Rhinoceros unicornis* the cusps are rounded and blunt, and mostly low. Conversely, in the Recent browser species *Diceros bicornis*, *Dicerorhinus sumatrensis*, and *R. sondaicus* the cusps are mainly high and sharp or rounded, which is also true of the cusps in the fossil species *Stephanorhinus hundheimensis* and *S. kirchbergensis*. The fossil species *S. hemitoechus* in turn differs from Recent browsers in that the cusps are mostly rounded, with some blunt and sharp cusps present as well. In hierarchical cluster analysis the browsers, including the Recent species *R. sondaicus*, *D. sumatrensis*, and *D. bicornis* as well as the fossil species *S. hundsheimensis* and *S. kirchbergensis*, form a separate group. Another group is formed by the species *R. unicornis*, *C. antiquitatis*, and *C. simum*, all of whose diet is more abrasive. The species *S. hemitoechus* falls between these two main groups in the analysis.

In Figure 7 we display the data obtained from the mesowear analysis of the upper molars, with the data factored according to roundedness in Figure 7.1 and according to height in Figure 7.2. With respect to both of these factors separately, the browsers *D. bicornis*, *D. sumatrensis*, *R. sondaicus*, *S. hundsheimensis*, and *S. kirchbergensis* clearly form a group, which is separated from the species *S. hemitoechus*. Thus we conclude that the cusps are, on average, both lower and more rounded in the species *S. hemitoechus* than in browsers. On the other hand, the species *C. antiquitatis* in turn falls between the extreme grazer *C. simum* and the graze-dominated mixed-feeder *R. unicornis*, which suggests that its cusp apices are, on the average, not as low or as blunt as in *C. simum*.

The data obtained from the analyses of the lower molars are displayed in Figures 8 and 9. The angles between the enamel edges and the buccal surfaces as measured in the hypoconid, and protoconid tip regions are shown in Figure 8. The angles are clearly larger on the average for the browsers *D. bicornis*, *D. sumatrensis*, *R. sondaicus*, *S. hundsheimensis*, and *S. kirchbergensis* than for other species. Thus these browsers form a clearly separate group. The angles related to the species *S. hemitoechus* are somewhat smaller. On the average, the smallest angles were those measured from the molars of the Recent grazer *C. simum*, whereas the average of the angles of the species *C. antiquitatis* were smaller than the average of the angles of the Recent mixed feeder *R. unicornis*.

In Figure 9.1 we show the data obtained when we classified the lower molars into five groups according to the number of facets on the buccal side of the enamel edge. Figure 9.2 in turn shows

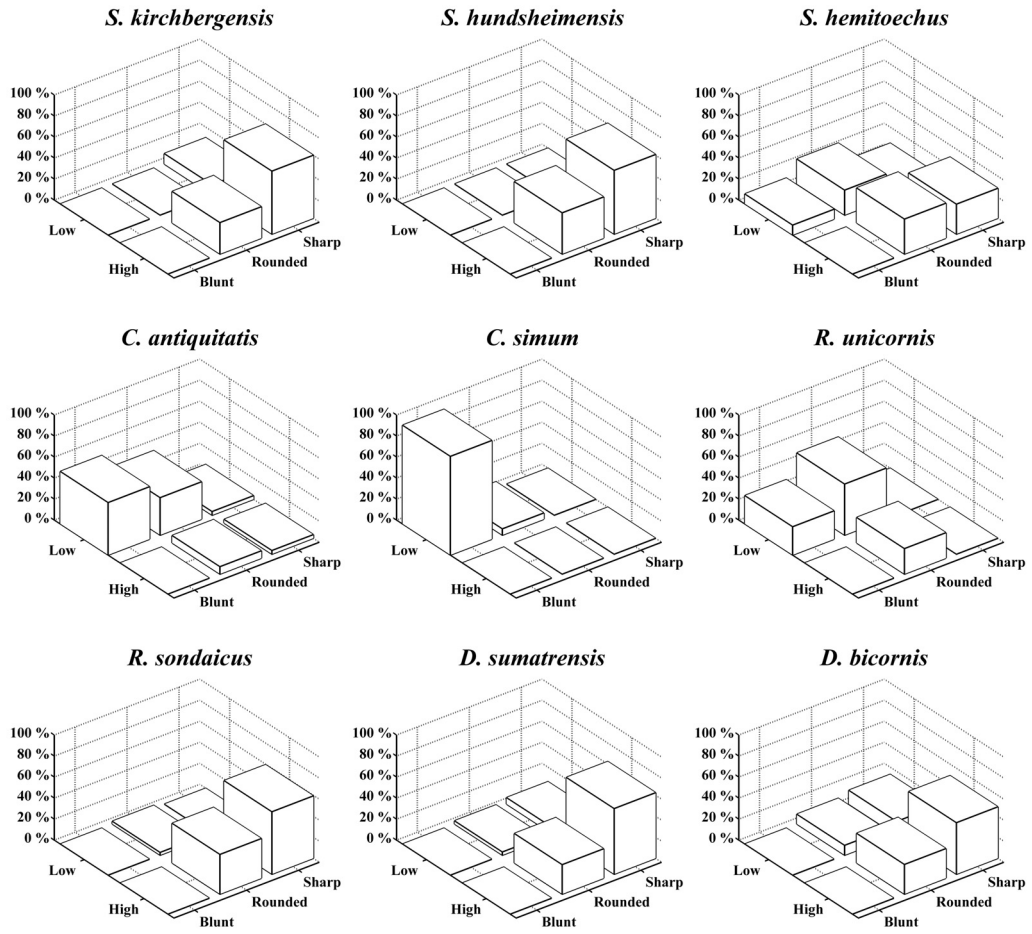

FIGURE 5. Bivariate bar plot of mesowear data of the upper molars M2 and M1, to show the combined distribution of occlusal relief and cusp roundness. From left to right, the height of the bars in the back row represent the percentage of cusps which are: low and blunt, low and rounded, low and sharp, and the bars in the front row represent the percentage of cusps which are: high and blunt, high and rounded, high and sharp.

the data obtained with the simpler variation of the method, where the molars were classified into two groups according to whether they have facets or not. In both of these datasets the browsers clearly form a separate group, which is explained by well-developed facets. The species *S. hemitoechus* presents facets on most molars, the mixed feeder *R. unicornis* presents some facets, whereas the grazer *C. simum* does not present facets at all. Once again, the species *C. antiquitatis* falls between the species *C. simum* and *R. unicornis*.

It is rather laborious to manually measure the angle of the enamel edge and, contrary to mesowear analysis, it cannot therefore be used to process large numbers of samples “at a glance.” Therefore we also investigated whether the lower molars could be analysed by a fast visual method. The only feature that can be determined with sufficient rapidity and simplicity for our purposes is whether or not the buccal side enamel edge of a lower molar does or does not have facets. We applied this idea in two different ways. In the first case we studied separately the lack or existence of the facets one, two, six, and seven, and counted the total number of facets present. Hence we arrived at a number between 0 and 4, with 0 indicating no facets and 4 indicating that facets are present everywhere on the enamel edge. The results we obtained with this method (Figure 9.1) match the results obtained by mesowear analysis of upper molars (Figure 7). The second analysis we applied was even simpler. There we classified the lower molars into two groups according to whether they have buccal side facets or not. As can be seen from Figure 9.2, the data obtained by this analysis also allow us to separate browsers,

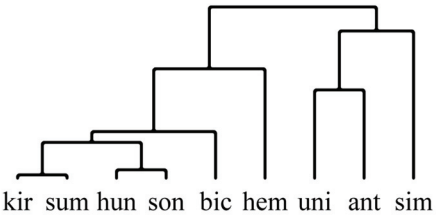

FIGURE 6. Hierarchical cluster analysis of the upper molars M2 and M1. ant=*C. antiquitatis*, bic=*D. bicornis*, hem=*S. hemitoechus*, hun=*S. hundsheimensis*, kir=*S. kirchbergensis*, sim=*C. simum*, son=*R. sondaicus*, sum=*D. sumatrensis*, uni=*R. unicornis*.

mixed feeders, and grazers from each other. The benefit of this particular analysis is that it is easy to use and fast, but it is slightly less accurate than the other analyses considered here. Its accuracy is sufficient for browsers and grazers to be discriminated from each other, but it places the species *S. hemitoechus* close to the browsers as only one of the studied molars was completely facetless. On the other hand, as the other analyses studied, it is able to separate the Recent mixed feeder *R. unicornis* from the grazer *C. simum* and the browsers, and the species *C. antiquitatis* from the species *C. simum* and *R. unicornis*.

DISCUSSION

As our results show, the presented method for obtaining 3D models from sets of (ordinary) photographs seems to be well suited for palaeontological work. We note that the models obtained by the method are at least sufficiently accurate for the study of the buccal side facets of lower molars of rhinoceroses, although these facets are only about 1-5 mm wide. Hence it is clear that the method will be suitable for many other palaeontological studies as well. A clear benefit of the presented method is that research that requires 3D models can now be performed by almost anyone with a digital camera and a computer, without the need to access expensive and often difficult-to-use 3D scanners. In particular, we note that the simplicity and speed of photography means that some research, which has traditionally had to be done in situ at museums, often under severe time constraints, can with this technique be deferred to off-site investigations of the generated 3D models. We also note that it is, at least in principle, possible to use a digital video camera to even more conveniently obtain the image sequences by extracting individual frames from the recorded movie.

We found that with the generation of 3D reconstruction software we used, the most important aspect of obtaining good 3D models was to have sharp photographs. This is easy to understand when comparing the level of detail found out-of-focus regions of photographs to the level of details in regions that are in focus, as the latter obviously contains more information. In our case this meant that the out-of-focus parts of the photographs had to be masked out by hand. Undoubtedly, once the art of obtaining 3D models from 2D photographs matures, this step will become unnecessary.

We observe that the measured angle between the buccal side enamel edge and the buccal side

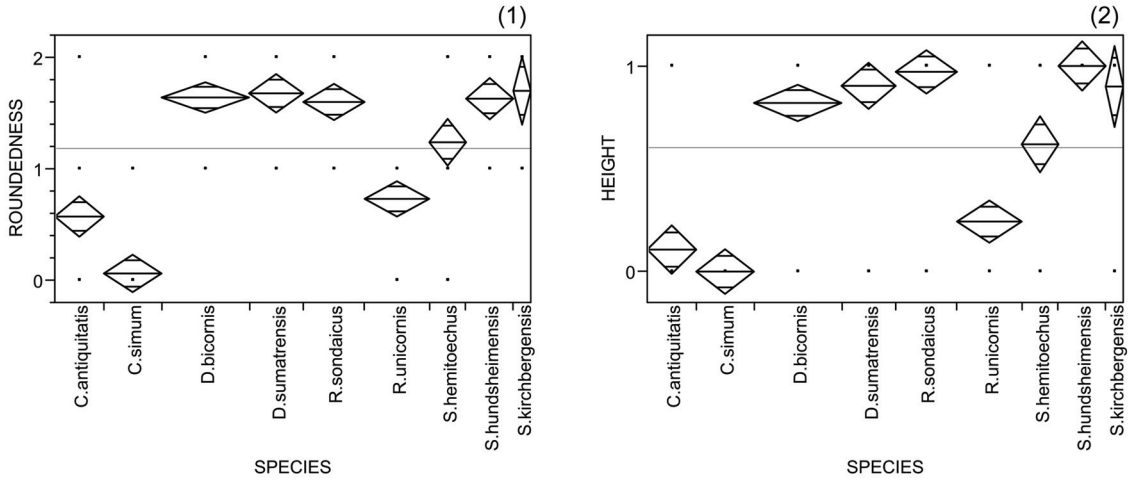

FIGURE 7. Mesowear data of the upper molars M2 and M1. 1. Cusp apices scored by roundedness: 0=blunt cusps, 1=rounded cusps, 2=sharp cusps. 2. Cusp apices scored by height: 0=low cusps, 1=high cusps.

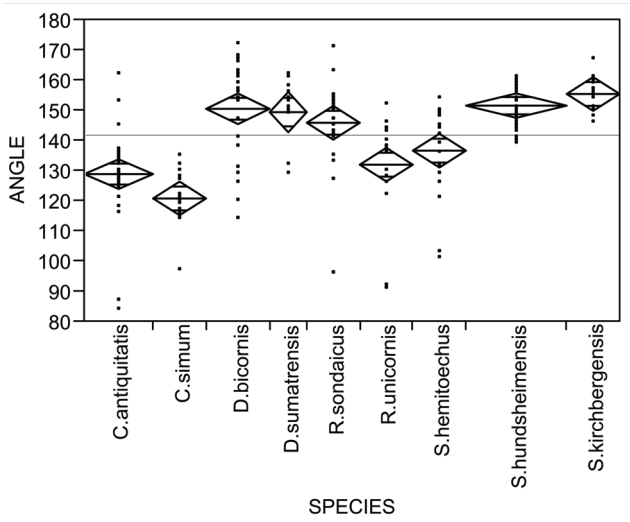

FIGURE 8. The angles between the buccal surface and buccal side enamel edge of the lower molars m2 and m1.

surface is much larger in those molars with a facet than in those molars with no facets. Hence large average angles seem to generally suggest attrition, whereas small average angles generally suggest abrasion. When the average angles are compared to the upper molar mesowear of the same species, we observe that for browsing species, for which the cusps are on the average high and sharp, the angles are also on the average larger. On the other hand, small average angles seem to correlate well with the low and blunt cusps of grazers. Furthermore, the results obtained for mixed-feeders from the lower molars match those obtained from the upper molars.

There are, however, drawbacks to using the measured angles as attributes of wear. First of all, there are differences in the morphology of the buccal side surfaces in different species, but in this work the angles were measured with respect to these surfaces, with the assumption that the surfaces have a fixed direction. This, however, represents an oversimplification of reality since the curvature, or flatness, of the buccal side surface depends on the morphology of each species. To some extent it is possible to attribute convex buccal side surfaces to browsing species, whereas grazing species have a more vertical buccal side surface. This morphological difference leads to a slight exaggeration of the difference between the measured angles of browsers and grazers. Indeed, the convex buccal side surface found in browsers tends to lead to a slight increase in the measured angle, whereas the straight buccal side surface of grazers tends to slightly decrease the measured angle. It could be possible to eliminate this problem by using, instead of the buccal side surface, some other surface of a tooth, such as for example the growth-direction of the molar roots, as was done by Butler (1972) in a different context. However, since it is difficult to determine in what directions the molar roots grow when studying teeth still attached to the skull, we decided to exclusively use the buccal side surface as reference.

Although it is typically straightforward to consistently measure the enamel edge angle, in some cases it can happen that the facet or the enamel edge itself is convex. In such cases the measurement can be tried at a slightly different location, which usually solves the problem. Otherwise it may be necessary to apply experience to get a reasonable estimate of the angle. We have encountered such difficult cases mainly with teeth from mixed feeders, and the number of such cases is, in any case, so low that they should only slightly affect the obtained results. When we assessed the repeatability of the method by measuring the angle at the hypoconid tip of a single tooth at 10 separate occasions, we found that the difference between the largest and the smallest result deviated by only 2.8 degrees. Since the difference between the largest and the smallest angles of the measured teeth was over 80 degrees, we are therefore confident that, although the deviation when measuring a particular tooth might be larger than 2.8 degrees, the method yields angle measurements, which are sufficiently accurate for our purposes.

We have previously used lower molar mesowear, based on facet development, to study

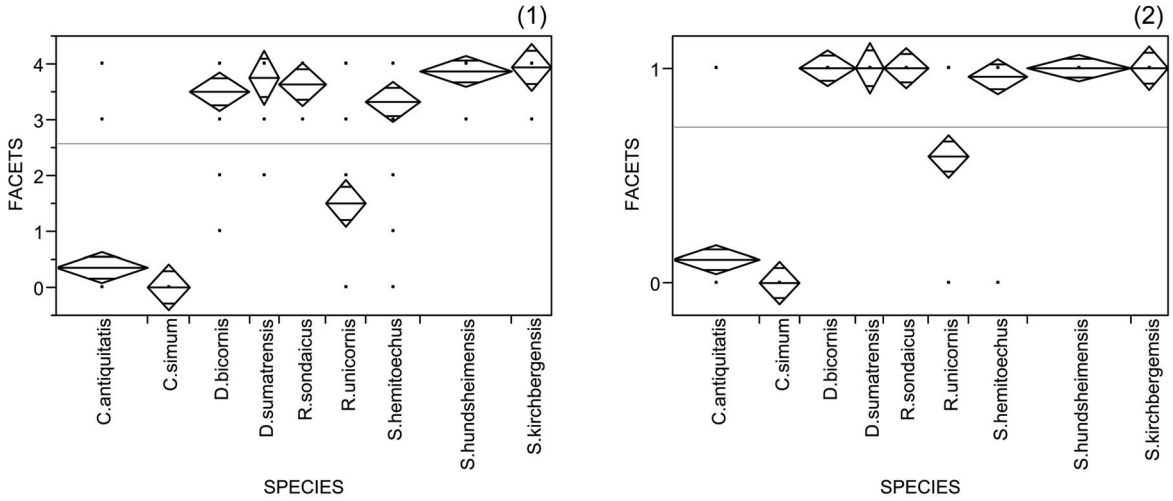

FIGURE 9. Mesowear data of the lower molars m2 and m1. Data obtained from the visual analysis, 1. facets analysed separately: 0=no facets, 1=one facet, 2=two facets, 3=three facets, 4=four facets, 2. only presence of facet analysed: 0=no facet, 1=at least one facet.

the palaeodiet in the Pliocene species *Ceratotherium efficax* (Dietrich, 1942) in the Laetoli region in Tanzania (Hernesniemi et al. 2011). In that study the lower molars were divided into three groups; those with no facets (corresponding to blunt upper molars), those with facets with fuzzy boundaries (corresponding to rounded upper molars), and those with facets with sharp boundaries (corresponding to sharp upper molars). In the present study we noticed that the fuzzy boundary is not a very reliable factor, and accordingly proceeded to simplify the classification into molars with facets and molars without. Such a classification does not allow direct identification with upper molar classification and must therefore be separately analysed. However, as Franz-Odentaal and Kaiser (2003) observed from ruminants, the data obtained from the mesowear analysis of the lower teeth tends to be more rounded than the correspondent data from upper teeth. Kaiser and Fortelius (2003) suggested that due to gravity the matter being chewed is in more contact with lower molars than with upper molars, which could explain the differences observed in the corresponding mesowears. Thus mixing upper and lower molars in the same analysis may be inappropriate in any case.

In this work we treated each fossil species as a single group, as all the studied dental fossils come from the fossil localities of Britain. Thus, the dietary regimes were studied at the species level, without a strict differentiation according to age or locality. However, as observed in the species *Stephanorhinus hundsheimensis* by Kahlke and Kaiser (2010), some intraspecific differentiation in dietary habits between populations are possible, especially since the Pleistocene palaeoenvironments were very variable.

CONCLUSIONS

In this work we evaluated how well 3D models reconstructed from ordinary photographs are suited for palaeontological investigations. As a test case we studied if an analysis of the buccal side enamel edge facets of the lower molars of rhinoceroses reveals information about the dietary regimes of these animals in the way mesowear analysis does. The reconstructed 3D models we obtained are consistent with models obtained by needle or laser scanners, although the achieved resolution is somewhat lower, resulting in a slight loss of detail of the models. However, the models were nevertheless sufficiently accurate to allow an investigation of the molar wear facets, which typically are just a few millimetres wide. Thus we are convinced that 3D models obtained from photographs are sufficiently accurate to provide the information necessary for many different palaeontological studies.

The shape of the enamel edge of the buccal lower molars varies greatly among the different species of rhinoceroses as illustrated in Figure 1. Most of this variation is explained by the differences in how the species feed. The amount of attrition and abrasion in the teeth of an animal depends on its diet and can therefore be used when trying to reconstruct palaeodiets. For upper molars the ratio

of the amounts of attrition and abrasion, which is determined by the degree of facet formation, can be estimated by classical mesowear analysis, where the sharpness and height of the buccal cusps are studied. In this work we studied if the lower molar wear facets in rhinoceroses can be similarly used to estimate the abrasiveness of the diet. The results we obtained in our test case seem to indicate that these facets are relatively well suited for estimating the abrasiveness of the diet. There appears to be a strong correlation between the data obtained from the lower molar facets (Figures 8, 9) with the data obtained from a mesowear analysis of the upper molars (Figure 7).

Of those species included as test cases in this study, the Pleistocene rhinoceros species *Stephanorhinus kirchbergensis* and *S. hundsheimensis* are browsers. The species *S. hemitoechus* seems to have been feeding on a diet that was slightly more abrasive than the diet of de facto browsing rhinoceroses, but notably less abrasive than the diet of the Recent graze-dominated mixed feeder *Rhinoceros unicornis*. Mesowear data places the woolly rhinoceros *Coelodonta antiquitatis* between *R. unicornis* and the extreme grazer *Ceratotherium simum*, which makes it a grazer, as expected. However, its diet was on the average not quite as abrasive as the diet of *C. simum*.

ACKNOWLEDGMENTS

We sincerely thank the curators and other staff of the following museums for access to specimens over decades; the British Museum of Natural History, London; the Finnish Museum of Natural History, Helsinki; the Zoological Museum, Natural History Museum of Denmark, Copenhagen; Koninklijk Museum voor Midden-Afrika, Tervuren, and the Museum of Evolution at Uppsala University. We would also like to thank R. Portela-Miguez, A. Currant, A. Karme, and I. Corfe for their help. Financial support for this study was provided to EH by the Alfred Kordelin Foundation. The study visits of EH (GB-TAF-5655 and DK-TAF-5605) received support from the SYNTHESYS Project (http://www.synthesys.info/), which is financed by European Community Research Infrastructure Action under the FP6 “Structuring the European Research Area” Programme.

REFERENCES

Billia, E.M.E. 2007. First records of *Stephanorhinus kirchbergensis* (Jäger, 1839) (Mammalia, Rhinocerotidae) from the Kuznetsk Basin (Kemerovo, Kuzbass area, South-East of Western Siberia). *Bollettino della Paleontologica Italiana*, 46:95-100.

Billia, E.M.E. 2008a. The skull of *Stephanorhinus kirchbergensis* (Jäger 1839) (Mammalia, Rhinocerotidae) from the Irkutsk region (Southwest Eastern Siberia). *Quaternary International*, 179:20-24.

Billia, E.M.E. 2008b. Revision of the fossil material attributed to *Stephanorhinus kirchbergensis* (Jäger 1839) (Mammalia, Rhinocerotidae) preserved in the museum collections of the Russian Federation. *Quaternary International*, 179:25-37.

Blumenbach, J.F. 1799. *Handbuch der Naturgeschichte* (Sechste Auflage). Dieterich, Goettingen.

Burchell, W.J. 1817. Note sur une nouvelle espèce de rhinocéros. *Bulletin des Sciences, par la Société Philomatique, Paris*, June 1817:96-97.

Butler, P.M. 1952. The milk-molars of Perissodactyla, with remarks on molar occlusion. *Proceedings of the Zoological Society of London*, 121:777-817.

Butler, P.M. 1972. Some functional aspects of molar evolution. *Evolution*, 26:474-483.

Desmarest, A.G. 1822. *Mammalogie ou description des espèces de mammifères. Encyclopèdie Mèthodique,* Agasse, Paris.

Dietrich, W.O. 1942. Zur Entwicklungsmechanik des Gebisses der afrikanischen Nashörner. *Zentralblatt für Mineralogie,* 1942:297-300.

Falconer, H. 1868. On the European Pliocene and Post-Pliocene Species of the Genus Rhinoceros, p. 309-403. In Murchison, C. (ed.), *Palaeontological Memoirs and Notes of the late Hugh Falconer*, Volume 2, Spottiswoode and Co., London.

Fischer, G. 1814. *Zoognosia: tabulis synopticis illustrata.* N. S. Vsevolozsky, Moscow.

Fortelius, M. 1982. Ecological Aspects of Dental Functional Morphology in the Plio-Pleistocene Rhinoceroses of Europe, p. 163-181. In Kurten, B. (ed.), *Teeth, Form, Function, and Evolution*. Columbia University Press, New York.

Fortelius, M. 1985. Ungulate cheek teeth: developmental, functional, and evolutionary interrelations. *Acta Zoologica Fennica*, 180:1-76.

Fortelius, M. and Solounias, N. 2000. Functional Characterization of Ungulate Molars Using the Abrasion-Attrition Wear Gradient: A New Method for Reconstructing Paleodiets. *American Museum Novitates*, 3301:1-36.

Fortelius, M., Mazza, P., and Sala, B. 1993. *Stephanorhinus* (Mammalia: Rhinocerotidae) of the western European Pleistocene, with a revision of *S. etruscus* (Falconer, 1868). *Palaeontographica Italica*, 80:63-155.

Franz-Odentaal, T.A. and Kaiser, T.M. 2003. Differential mesowear in the maxillary and mandibular cheek dentition of some ruminants (Artiodactyla). *Annales Zoologici Fennici*, 40:395-410.

Furukawa, Y. and Ponce, J. 2007. Accurate, Dense, and Robust Multi-View Stereopsis. *IEEE Computer Society Conference on Computer Vision and Pattern Recognition*. http://www.cs.washington.edu/homes/furukawa/papers/cvpr07a.pdf

Gray, J.E. 1868. Observations on the preserved specimens and skeletons of Rhinocerotidae in the collection of the British Museum and Royal College of Surgeons, including the description of three new species. *Proceedings of the Zoological Society of London* (for 1867):1003-1032.

Groves C.P., Fernando, P., and Robovský J. 2010. The Sixth Rhino: A Taxonomic Re-Assessment of the Critically Endangered Northern White Rhinoceros. *PLoSONE*, 5:e9703. doi:10.1371/journal.pone.0009703

Hernesniemi, E., Giaourtsakis, I.X., Evans, A.R., and Fortelius, M. 2011. Rhinocerotidae, p. 275-294. In Harrison, T. (ed.), *Paleontology and geology of Laetoli, Tanzania: human evolution in context. Volume 2: Fossil hominins and the associated fauna*. Springer, Dordrecht.

Jäger, G.F. 1835-39. *Über die fossilen Säugetiere welche in Württemberg in verschiedenen Formationen aufgefunden worden sind, nebst geognotischen Bemerkungen über diese Formtionen.* C. Erhard Verlag, Stuttgart.

Janis, C.M. 1988. An estimation of tooth volume and hypsodonty indices in ungulate mammals and the correlation of these factors with dietary preferences, p. 367-387. In Russel, D.E., Santorio, J.P., and Signogneu-Russel, D. (eds.), *Teeth revised: proceedings of the VII international symposium on dental morphology.* Muséum national de Histoire Naturelle Memoir série C.

Kahlke, R.-D. and Kaiser, T.M. 2010. Generalism as a subsistence strategy: advantages and limitations of the highly flexible feeding traits of Pleistocene *Stephanorhinus hundheimensis* (Rhinocerotidae, Mammalia). *Quaternary Science Reviews*.

Kahlke, R.-D. and Lacombat, F. 2008. The earliest immigration of woolly rhinoceros (*Coelodonta tologoijensis*, Rhinocerotidae, Mammalia) into Europe and its adaptive evolution in Palaearctic cold stage mammal faunas. *Quaternary Science Reviews*, 27:1951-1961.

Kaiser, T.M. and Fortelius, M. 2003. Differential Mesowear in Occluding Upper and Lower Molars: Opening Mesowear analysis for Lower Molars and Premolars in Hypsodont Horses[JENNIFER: shouldn't this title be only in initial caps?]. *Journal of Morphology*, 258:67-83.

Kaiser, T.M. and Rössner, G.E. 2007. Dietary resource partitioning in ruminant communities of Miocene wetland and karst palaeoenvironments in Southern Germany. *Palaeogeography, Palaeoclimatology, Palaeoecology*, 252:424-439.

Kaiser, T.M. and Solounias, N. 2003. Extending the tooth mesowear method to extinct and extant equids. *Geodiversitas*, 25:321-345.

Koenigswald, W.v.[JENNIFER: is this author name "von Koenigswald? Seems like I've seen that before and if so, it should be moved alpha.], Smith, B.H. and Keller, T. 2007. Supernumerary teeth in a subadult rhino mandible (*Stephanorhinus hundsheimensis*) from the middle Pleistocene Mosbach in Wiesbaden (Germany). *Paläontologishe Zeitschrift*, 81:416-428.

Kretzoi, M. 1942. Präokkupierte und durch ältere zu ersetzende Säugetiernamen. *Földtani Közlöny*, 72:345-349.

Lacombat, F. 2006a. Pleistocene Rhinoceroses in Mediterranean Europe and in Massif Central (France). *Courier Forschungsinstitut Senckenberg,* 256:57-69.

Lacombat, F. 2006b. Morphological and biometrical differentiation of the teeth from Pleistocene species of Stephanorhinus (Mammalia, Perissodactyla, Rhinocerotidae) in Mediterranean Europe and the Massif Central, France. *Palaeontographica Abteilung (A (Paläozoologie—Stratigraphie*), 274:71-111.

Lacombat, F. 2007. Phylogeny of the genus Stephanorhinus in the Plio-Pleistocene of Europe. *Hallesches Jahrbuch fûr Geowissenschaften,* 23:63-64.

Linnaeus, C. 1758. *Systema Naturae. I: Regnum Animale* (10th edition). Stockholm.

Loose, H. 1975. Pleistocene Rhinocerotidae of W. Europe with reference to the recent two-horned species of Africa and S.E. Asia. *Scripta Geologica*, 33:1-59.

Mazza, P. 1988. The Tuscan Early Pleistocene rhinoceros *Dicerorhinus etruscus*. *Palaeontographica Italica*, 75:1-87.

Snavely, N., Seitz, S.M., and Szeliski, R. 2006. Photo Tourism: Exploring photo collections in 3D, ACM Transactions on Graphics. *Proceedings of SIGGRAPH*.

Tong, HW. and Wu, XZ. 2010. *Stephanorhinus kirchbergensis* (Rhinocerotidae, Mammalia), from the Rhino Cave in Shennongjia, Hubei. *Chinese Science Bulletin*, 55:1157-1168.

Toula, F. 1902. Das Nashorn von Hundsheim *Rhinoceros* (*Ceratorhinus* Osborn) *hundsheimensis* nov. form. mit Ausführungen über die Verhältnisse von elf Schädeln von *Rhinoceros* (*Ceratorhinus*) *sumatrensis*. *Abhandlungen der Kaiserlich-Königlichen Geologischen Reichsanstalt*, 57:445-454.

Zeuner, F.E. 1934. Die Beziehungen zwischen Schädelform und Lebenweise bei den rezenten und fossilen Nashörnern. *Berichte der Naturforschenden Gesellschaft zu Freiburg*, 34:21-79.

APPENDIX

Dental material used in this study

Recent species:

***Diceros bicornis*:** BMNH-1948.1.28.4 BMNH-1948.1.28.5 BMNH-1948.1.28.7 BMNH-1962.7.6.5 BMNH-1962.7.6.6 BMNH-25.7.6.1 BMNH-7.2.26.1BMNH-84.8.1.1 FMNH-647/1960 FMNH-944/1960 FMNH-945/1960 NHMD-CN1653 NHMD-CN1703 NHMD-CN26 NHMD-CN2653 NHMD-CN2999 NHMD-CN3695 NHMD-CN3729 RMCA-RG7987

Ceratotherium simum: BMNH-1851.12.23.1 BMNH-1964.8.31.4 BMNH-1967.8.31.2 BMNH-1967.8.31.3 BMNH-1967.8.31.5 BMNH-1976.209 BMNH-25.5.23.1 BMNH-30.7.26.1 BMNH-52.12.9.1 NHMD-CN2662 RMCA-RG5925

***Rhinoceros sondaicus*:** BMNH-1861.3.11.1 BMNH-1932.10.21.1 BMNH-1951.11.30.4 BMNH-20.10.13.1 BMNH-51.11.10.11 BMNH-72-721 BMNH-76.3.30.1 BMNH-79.11.21.178 FMNH-704 NHMD-CN27 NHMD-CN28 NHMD-CN29 NHMD-CN3320 NHMD-CN524

***Rhinoceros unicornis*:** BMNH-1.3.10.1 BMNH-1884.1.22.1+2 BMNH-1903.2.13.1 BMNH-1926.6.7.8 BMNH-1950.10.18.5 BMNH-1951.11.30.2 BMNH-47.12.20.2 BMNH-72.12.30.1 BMNH-72.739 BMNH-83.10.23.3 NHMD-CN25 UUZM-no-number

***Dicerorhinus sumatrensis*:** BMNH-1.1.22.1 BMNH-1461a BMNH-1879.6.14.2 BMNH-1894.9.24.1 BMNH-1921.2.8.2 BMNH-1921.2.8.4 BMNH-1948.1.14.2 BMNH-1948.12.20.1 BMNH-1949.1.11.1 BMNH-54.8.16.1 BMNH-72.12.31.1 NHMD-CN617

Pleistocene species:

***Coelodonta antiquitatis*:** Aylesford, Kent: BMNH-34819 M2s, BMNH-34819 M1s, BMNH-34819 M2d, BMNH-no-number M2s, BMNH-no-number m2s. Batheaston, Somerset: BMNH-44741 M1s, BMNH-44741 M2s. Bedford, Bedfordshire: BMNH-M.5167 M1d, BMNH-M.5606 M1d, BMNH-M.5606 M2s, BMNH-M.5607 m2s. Brixham Cave, Torquay, Devon: BMNH-48498 M1s, BMNH-48499 m1s, BMNH-48500 m1d, BMNH-48513 m, BMNH-48525 m2d, BMNH-48526 m1s, BMNH-48527 M2d, BMNH-48528 m2s, BMNH-48533 m1s. Cats Hole Cave, Gower: BMNH-M.87 M2s, BMNH-M.89 m2s. Chartham, Canterbury, Kent: BMNH-M.82184 M2d. Crayford, Kent: BMNH-38721 M1d, BMNH-M.5118 m2d, BMNH-M.5125 M2s, BMNH-M.5125 M2s, BMNH-M.5125 M2s. Hackney Wick Pit, Hackney: BMNH-no-number m1s. Ightham, Kent: BMNH-M.11794 M2s. Kents Cavern, Devon: BMNH-4750 m2s, BMNH-4842 m1d, BMNH-4890 m1s, BMNH-k.c.12.11.1934 m2s, BMNH-k.c.12.12.1938 m2d, BMNH-k.c.15.1.1940 m2d, BMNH-k.c.19.5.1930 m1d, BMNH-k.c.29.1.1940 m1d, BMNH-k.c.29.3.1937 m1s, BMNH-k.c.3.11.1930 m1s, BMNH-k.c.30.1.1039 m2d, BMNH-k.c.5.12.1938 m1d, BMNH-k.c.8.1.1940 m2d, BMNH-no-number m2d, BMNH-no-number M1d, BMNH-no-number M2s, BMNH-no-number M2s. King Arthurs Cave, Hereford: BMNH-42041 M1s, BMNH-42042 m2s, BMNH-no-number m1d, BMNH-no-number m1d. Lavenham, Suffolk: BMNH-M.5590 m1d. Lea Valley, Edmonton: BMNH-16800 m1d, BMNH-16800 m2d. Peterborough, Cambridgeshire: BMNH-M.9130 M1s, BMNH-M.9130 M1d. Possibly from the North Sea: BMNH-no-number m1s. Torbryan Cavern, Torquay, Devon: BMNH-M.4642 m1s, BMNH-4642 m2d. Whitefrials st., London: BMNH-M.8585 m2s. Whitemoor Haye Pit, Staffordshire: BMNH-no-number M2d, BMNH-no-number M2s, BMNH-no-number M1s, BMNH-no-number M1d, BMNH-no-number m2s, BMNH-no-number m2d. Wookey Hole caves, Somerset: BMNH-M.242 m1s, BMNH-M.242 m2d. Unknown: BMNH-47111 M1d, BMNH-47111 M1s.

***Stephanorhinus hundsheimensis*:** Norfolk Coast: BMNH-33324 M1s, BMNH-33324 M2d, BMNH-no-number M1d. Palling, Norfolk: BMNH-18475 m1s, BMNH-18475 m1d, BMNH-18475 m2s, BMNH-18475 m2d. Sidestrand, Norfolk: BMNH-M.19427 m1s, BMNH-M.19436 m1d, BMNH-M.1936 m2d, BMNH-M.19440 m1s, BMNH-M.19440 M2s, BMNH-M.19445 m1d, BMNH-M.1945 m2d, BMNH-M.19465 M1s, BMNH-M.19465 M2s, BMNH-M.19478 m1d, BMNH-M.1948 m1d, BMNH-M.1948 m2d, BMNH-M.6109 m1s, BMNH-6109 m1d, BMNH-6109 m2s, BMNH-M.6633 m1d, BMNH-M.6633 m2d, BMNH-6639 m2d, BMNH-6663 M2d, BMNH-6668 m2s. Trimmingham, Norfolk: BMNH-M.18496 m2s, BMNH-M.19426 m2s, BMNH-M.19428 m1d, BMNH-M.19428 m2d, BMNH-M.19429 m2d, BMNH-M.19430 m1s, BMNH-M.19431 m2s, BMNH-M.19432 m2s, BMNH-M.19434 m2s, BMNH-M.19435 m1d, BMNH-M.19435 m2d, BMNH-M.19437 m2d, BMNH-M.19444 m1s, BMNH-M.19444 m2s, BMNH-M.19446 m1d, BMNH-M.19446 m2d, BMNH-M.19447 m2d, BMNH-M.19456 M2s, BMNH-M.19457 M2d, BMNH-

M.19458 M2s, BMNH-M.19458 M1s, BMNH-M.19459 M1s, BMNH-M.19481 m1d, BMNH-M.19483 m2s, BMNH-M.19492 M1s, BMNH-M.19492 M2s, BMNH-M.19493 M2d, BMNH-M.19493 M1d, BMNH-M.19498 M1s, BMNH-M.19498 M2s, BMNH-M.19498 M2d, BMNH-M.19499 M2d, BMNH-M.19499 M1s, BMNH-M.19499 M1d, BMNH-M.19499 M2s, BMNH-M.19504 M1s, BMNH-M.6628 m2d, BMNH-M.6629 m2s, BMNH-6632 M1s, BMNH-M.6632 M1d, BMNH-M.6632 M2s, BMNH-M.6632 M2d, BMNH-M.6653 M2s, BMNH-M.6658 M2d, BMNH-M.6667 m1d. Westbury Quarry, Westbury-sub-Mendip, Somerset: BMNH-M.33773 M1s, BMNH-M.33773 M2s.

***Stephanorhinus hemitoechus*:** Crayford, Kent: BMNH-M.5119 m2s. East Mersea, Essex: BMNH-M.20457. Grays, Essex: BMNH-18755-m1d, BMNH-18755 m2d, BMNH-18793 M2d, BMNH-18799 m1d, BMNH-19799 m2s, BMNH-18755a M1s. Waterhall farm, Hertfordshire: BMNH-no-number M2s, BMNH-no-number m2s. Ilford, Essex: BMNH-45205 M2s, BMNH-45205 M2d, BMNH-45205 M1d, BMNH-45205 M1s, BMNH-45209 M2s, BMNH-45210 M1d, BMNH-45214 m1s, BMNH-45214 m1d, BMNH-45214 m2s, BMNH-45214 m2d, BMNH-45218 m2s, BMNH-45219 m1s, BMNH-45221 m1d, BMNH-45235 M1d, BMNH-45237 M1/2, BMNH-M.2771 m1d, BMNH-no-number M2s. Joint Mitnor Cave, Buckfastleigh, Devon: BMNH-no-number m1s, BMNH-no-number m2s. Lexden. Essex: BMNH-37404 M2s, BMNH-37404 M2d, BMNH-37405 m2d, BMNH-37406 m2s. Minchin Hole, Gower: BMNH-40938 M1d, BMNH-40938 M2d, BMNH-40939 M2s, BMNH-40939 M1s, BMNH-40942 m1s, BMNH-40942 m2s, BMNH-40943 m1d, BMNH-40943 m2d, BMNH-40944 m2s, BMNH-40946 M2d. Selsey, West Sussex: BMNH-M.36620 m1d, BMNH-M.36620 m2d. Swale Cliff, Kent: BMNH-M.34369 M1d, BMNH-M.34369-M2d. Thames Valley: BMNH-18795 M2d. Torbryan Cavern, Torquay, Devon: BMNH-M.4641 M2d. Tornewton Cave, Devon: BMNH-M.40335 m1d, BMNH-M.40336 m1d.

***Stephanorhinus kirchbergensis*:** Barnfield Pit, Swanscombe, Kent: BMNH-M.16158 m2d, BMNH-M.18967 M2s. Crayford, Kent: BMNH-M.5132 M2s. Grays, Essex: BMNH-2183 m2s, BMNH-18794 M1d, BMNH-18799 m2d, BMNH-19834 m2s, BMNH-19840 m1d, BMNH-19840 m2d, BMNH-19841 m2s, BMNH-19841 M2s, BMNH-20249 M2s, BMNH-22020 M1d, BMNH-22020 M2d, BMNH-22021 M1s, BMNH-40812 m1s, BMNH-40812 m2s, BMNH-19840a m1s, BMNH-19840a m2s. Ilford, Essex: BMNH-45283 M2s, BMNH-45284 M1s, BMNH-45285 m1s, BMNH-45285 m1d, BMNH-45285 m2s, BMNH-45285 m2d. West Thurrock, Essex: BMNH-39348 m1s, BMNH-39348 m2s.